Photoassociation spectroscopy of $^{87}Rb_2$ $(5s_{1/2}+5p_{1/2})0_g^-$ long-range molecular states: Analysis by Lu-Fano graph and improved LeRoy-Bernstein formula

H. Jelassi, B. Viaris de Lesegno, and L. Pruvost
Laboratoire Aimé Cotton, CNRS II, batiment 505, Campus d'Orsay, 91405 Orsay Cedex, France
(Received 29 July 2005; published 2 March 2006)

We report on cold atom photoassociation of ^{87}Rb giving spectroscopy data of the $(5s_{1/2}+5p_{1/2})0_g^-$ long-range molecular states in the asymptotic range of [−12.5 cm^{-1}, −1.5 cm^{-1}] below the dissociation limit. Using a Lu-Fano approach to analyze the data, we show that an improved LeRoy-Bernstein model has to be applied. This approach lets us determine the phase shift of the wave function at the dissociation limit of the 0_g^- series.

DOI: 10.1103/PhysRevA.73.032501 PACS number(s): 33.20.Tp, 32.80.Pj

I. INTRODUCTION

The photoassociation of cold atoms, proposed 1987 [1] and experimentally demonstrated in 1993 [2], has become a precise and powerful technique for molecular spectroscopy [3]. It allows the detailed analysis of long-range molecular states. Especially for the alkali-metal dimers, this technique is fruitful for the molecular states belonging to series which converge to the first $s+p$ dissociation limit. The molecular data, deduced from the photoassociation spectra, are mainly the energy of the bound states. These data are essential for the determination of the molecular parameters and therefore for the molecular curves.

In the case of cold atom photoassociation, many details can be deduced concerning the long-range part of the molecular potential. In the near-dissociation region, the molecular interaction is fully described by asymptotic laws and some models lead to a quite simple description of the observed molecular states. One of the models that is often applied was developed by LeRoy and Bernstein [4].

For the rubidium atom, a lot of experimental studies were reported, giving data for both isotopes. Available data mainly concern the molecular states belonging to series converging to the $5s_{1/2}+5p_{3/2}$ limit [5–9]. Only a few experimental data have been established for series converging to the $5s_{1/2}+5p_{1/2}$ limit for the isotope 85 [6,10–13] and isotope 87 [13,14]. In this paper, we present results of the photoassociation spectroscopy of ^{87}Rb atoms leading to molecular states of the $(5s_{1/2}+5p_{1/2})0_g^-$ series in the asymptotic range of $[-12.5cm^{-1}, -1.5cm^{-1}]$ below the dissociation limit.

In an usual point of view, the spectroscopy of the $^{87}Rb_2$ $(5s_{1/2}+5p_{1/2})0_g^-$ states presents many similarities with experimental works published for alkali-metal atoms: H_2 $(1s+2p)$ [15], Li_2 $(2s+2p_{1/2})$ [16,17], Na_2 $(3s+3p_{1/2})$ [18], K_2 $(4s+4p_{1/2})$ [19], and Cs_2 $(6s+6p_{1/2})$ [20–22]. The quantitative analysis of these spectroscopic data was done mainly by fitting with the LeRoy-Bernstein formula or by using numerical calculations of a RKR (Rydberg-Klein-Rees) potential.

In this paper, we examine the data with a different approach, which combines the LeRoy-Bernstein formula and the Lu-Fano approach. This approach, usually used for the Rydberg states, is very sensitive to any deviation of an assumed law. Here the deviation to the LeRoy-Bernstein formula allows us to value the required modification of the model. The Lu-Fano graph exhibits a linear variation of the quantum defect versus the energy, and is well interpreted by applying the recently proposed improved LeRoy-Bernstein formula [23].

The first section of the paper is devoted to the experiment, the presentation of spectra, and the deduced data. In the second part, the LeRoy-Bernstein approach is recalled, the potential curve is defined, and the Lu-Fano plot is presented and analyzed. The improved LeRoy-Bernstein formula is then applied to deduce the phase-shift parameter and the slope of the linear variation. These parameters, coupled to simple proposed analytic models, allow us to deduce some short-range potential characteristics, such as the location of the barrier and the minimum.

II. EXPERIMENT

The experiment is performed on ^{87}Rb atoms, trapped in a magneto-optical trap (MOT). The photoassociation is analyzed by applying the trap loss spectroscopy technique [24]. This method consists in recording the atom number while the photoassociation laser is frequency-scanned. If the laser wavelength is resonant to a molecular state, the photoassociation creates long-range excited molecules. These excited molecules, having a very short lifetime, rapidly desexcite either to molecules in a fundamental state or to fast atoms. In both cases, the produced species cannot be trapped in the MOT. Therefore, an atom loss is observed.

A general view of the experiment is presented in Fig. 1.

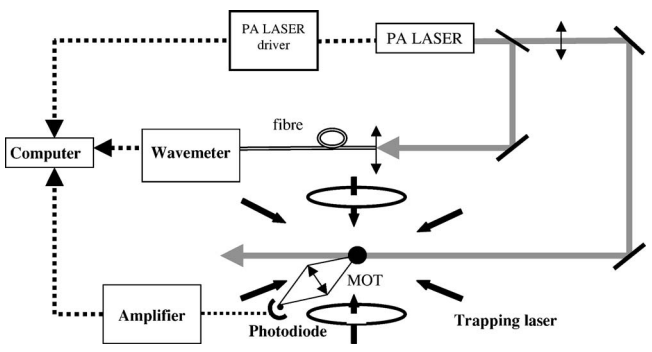

FIG. 1. Experimental setup.

 ©2006 The American Physical Society

The magneto-optical trap is produced in the ultrahigh-vacuum chamber made of nonmagnetic stainless steel. The background Rb pressure is in the 10^{-9} mbar range. The atom trap is created at the center of a quadripolar magnetic-field gradient, where three pairs of counterpropagating, retroreflected laser beams (8 mm diameter) in the standard σ^+/σ^- configuration orthogonally cross each other. In this region, the earth magnetic field and any other magnetic fields are compensated by using three pairs of Helmholtz coils. The lasers of the trap are provided by laser diodes (Hitachi and Sanyo) emitting about 50 mW laser power at $\sim$780 nm wavelength. The trapping laser is a Sanyo device having a linewidth about 1 MHz. It is frequency-locked near the rubidium line $5s_{1/2}F=2 \rightarrow 5p_{3/2}F'=3$, with a detuning of -2Γ (Γ being the natural linewidth of the $5p_{3/2}F'=3$ level, $\Gamma/2\pi=5.89$ MHz), by using a saturated absorption spectroscopy in an additional vapor cell. The repumping laser diode is a Hitachi model that is locked to the rubidium line $5s_{1/2}F=1 \rightarrow 5p_{3/2}F'=2$ via a similar method. Both lasers are superimposed and used to create the MOT.

With a quadripolar magnetic gradient of 14 G/cm and a few milliwatts per laser beam, cold clouds of $\sim 10^7$ atoms, with a $\sim$0.5 mm radius and 30 μK temperature, are usually created.

The photoassociation (PA) light is provided by a widely tunable titanium-sapphire laser (Coherent MBR 110) system with a typical output power of 900 mW and a linewidth of about 100 kHz. We use about 500 mW for the experiment. The PA laser beam is arranged in order to get a waist of 1 mm, slightly larger than the MOT size. The PA spectrum is obtained by scanning the PA laser wavelength and by simultaneously recording the cloud fluorescence, the fluorescence signal being proportional to the $5p_{1/2}F=2$ atom number in the trap. The fluorescence is collected onto a photodiode and the resulting signal is amplified to reach the volt range. The trap fluctuations are averaged numerically via the data acquisition (using a National Instrument card) of the amplified signal.

Simultaneously to the PA laser scanning, the laser wavelength is measured with a commercial wavemeter (Burleigh WA 1100) with an accuracy of 500 MHz ($\sim$0.01 cm^{-1}). The laser wavelength is recorded on a computer via a GPIB connection. A C^{++} program controls the different cards and stores the data in the computer with a repetition rate $\sim$4 Hz.

To explore the molecular states near the $5p_{1/2}$ limit, the PA wavelength is chosen to be red-detuned of the D_1 line at 795 nm. The PA laser is scanned automatically over 1 cm^{-1} (1 cm^{-1} during 600 s typically). Manual tunings are required to cover a wide range.

A typical photoassociation spectrum is shown in Fig. 2. The energy scale is presented relatively to the atomic transition $^{87}\mathrm{Rb}(5s_{1/2},F=2) \rightarrow {}^{87}\mathrm{Rb}(5p_{1/2},F'=2)$, whose energy is 12578.876 cm^{-1} [25]. The PA spectrum exhibits vibrational progressions corresponding to the 1_g, 0_u^+, and 0_g^- attractive molecular states. The states are identified by their energy spacing and width. In the range -12.5 cm^{-1} to -1.5 cm^{-1}, we have identified without any ambiguity 12 resonances belonging to the 0_g^- series. The found energy positions are reported in Table I. Results of 1_g and 0_u^+ states will be presented in detail in a future paper.

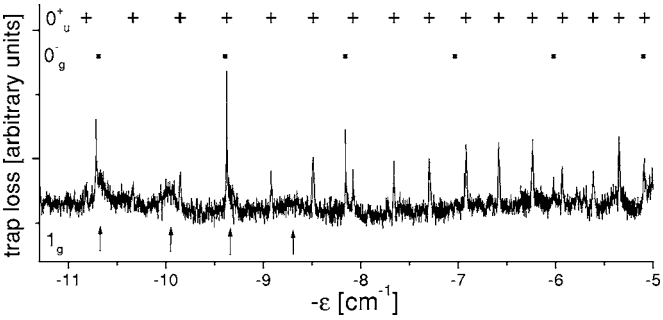

FIG. 2. Trap loss photoassociation spectrum recorded in the [-11.5 cm^{-1}, -5 cm^{-1}] below the dissociation limit: the crosses, squares, and arrows indicate the 0_u^+, 0_g^-, and 1_g level positions, respectively.

III. ANALYSIS OF THE DATA

Considering the energy range of the experimental study, which is typically -12.5 cm^{-1} to -1.5 cm^{-1} below the dissociation limit, the LeRoy-Bernstein formula is valid and can be applied in a first approximation. We propose then to couple this analysis to a Lu-Fano plot of the data. Such a plot, which is a differential method, allows us to evidence the difference in the LeRoy-Bernstein law and leads us to apply an improved LeRoy-Bernstein formula.

A. The LeRoy-Bernstein formula

The LeRoy-Bernstein formula [4] has been obtained in the case of an asymptotic molecular potential $V(R)=D-c_n/R^n$, with $n \geqslant 3$, with R the internuclear distance, D the dissociation limit, and c_n the multipole expansion coefficient. The starting point is the application of the Bohr-Sommerfeld rule for a bound vibrational molecular level v with the energy E,

TABLE I. $^{87}\mathrm{Rb}(5s_{1/2}+5p_{1/2})0_g^-$ levels: experimental energy positions measured relative to the atomic transition $^{87}\mathrm{Rb}(5s_{1/2},F=2) \rightarrow {}^{87}\mathrm{Rb}(5p_{1/2},F'=2)$ at 12578.876 cm^{-1}. The v values have been numerically determined by Dulieu [26].

v	Energy position (cm^{-1})
187	-12.173; -12.167; -12.167
188	-10.713; -10.713; -10.717; -10.716
189	-9.390; -9.397; -9.376; -9.375; -9.3750; -9.374
190	-8.147; -8.157; -8.156
191	-7.034
192	-6.019; -6.020
193	-5.098; -5.088
194	-4.292; -4.289; -4.280; -4.284; -4.272
195	-3.562; -3.564; -3.569; -3.563; -3.563
196	-2.909; -2.910; -2.925; -2.925; -2.925
197	-2.376; -2.359; -2.376; -2.368; -2.364; -2.379
198	-1.861; -1.879; -1.875; -1.873

TABLE II. C_3 coefficients for ^{87}Rb deduced from referenced data [an asterisk denotes using the nonrelativistic relation $C_3=(3\hbar/4\tau)(\lambda/2\pi)^3$].

Data	References	Year	C_3 (a.u.)
$\tau(5p_{3/2})=26.24(4)$ ns	[27,28]	1996	8.934(14)*
$\tau(5p_{3/2})=26.20(9)$ ns	[29,28]	1998	8.948(31)*
$\tau(5p_{1/2})=27.70(4)$ ns	[27,25]	1996	8.952(13)*
$\tau(5p_{1/2})=27.64(4)$ ns	[29,25]	1998	8.971(13)*
$M^2=8.688(25)\times10^5$ cm^{-1} Å^3	[30]	2002	8.905(26)
$M^2=8.799$ cm^{-1} Å^3	[30]	2002	9.0185
$M_{3/2}=5.956$ a.u.	[31]	1999	8.868
$M_{1/2}=4.221$ a.u.	[31]	1999	8.908
$C_3=9.202$ a.u.	[32]	1995	9.202

$$\frac{\sqrt{2\mu}}{\hbar}\int_{R_-}^{R_+}\sqrt{E-V(R)}dR=\left(v+\tfrac{1}{2}\right)\pi$$

with μ the reduced mass, and R_- and R_+ the inner and outer classical turning points of the vibrational motion solving the equation $V(R)=E$. Due to the form (sometimes complicated) of the real potential $V(R)$, the integral $\beta=(\sqrt{2\mu}/\pi\hbar)\int_{R_-}^{R_+}\sqrt{E-V(R)}dR$ depends strongly on E and $V(R)$. Nevertheless, the differentiation of β,

$$\frac{d\beta}{dE}=\frac{dv}{dE}=\frac{\sqrt{2\mu}}{h}\int_{R_-}^{R_+}\frac{dR}{\sqrt{E-V(R)}},$$

which represents the level density, is dominated by its value in the range defined by $V(R)\simeq E$.

The first LeRoy-Bernstein approximation is the use of the asymptotic potential form $V(R)=D-c_n/R^n$, in the calculation of $d\beta/dE$. The second approximation is the extension of the integral for short values of R, allowing the limit $R_-=0$. By introducing the energy difference $\epsilon=D-E$, the density of levels is therefore

$$\frac{d\beta}{d\epsilon}=-\frac{\sqrt{2\mu}}{h}\int_0^{R_+}\frac{dR}{\sqrt{-\epsilon+c_n/R^n}}.$$

Considering that $R_+^n=c_n/\epsilon$ and introducing the variable $x=R/R_+$, one gets

TABLE III. C_6 coefficients for a rubidium atom.

Data	References	Year	C_6 (a.u.)
$C_6^{\Pi}=3.88(5)\times10^7$ cm^{-1} Å^6	[30]	2002	$C_6^{\Pi}=8.05(10)\times10^3$
$C_6^{\Pi}=8.047\times10^3$ a.u.	[32]	1995	$C_6^{\Pi}=8.047\times10^3$
$C_6^{\Sigma}=6.22(12)\times10^7$ cm^{-1} Å^6	[30]	2002	$C_3^{\Sigma}=12.91(25)\times10^3$
$C_6^{\Sigma}=12.05\times10^3$ a.u.	[32]	1995	$C_6^{\Sigma}=12.05\times10^3$

TABLE IV. C_8 coefficients for a rubidium atom.

Data	References	Year	C_8 (a.u.)
$C_8^{\Pi}=1.43(10)\times10^9$ cm^{-1} Å^8	[30]	2002	$C_8^{\Pi}=1.06(7)\times10^6$
$C_8^{\Pi}=1.132\times10^6$ a.u.	[32]	1995	$C_8^{\Pi}=1.132\times10^6$
$C_8^{\Sigma}=4.66(50)\times10^9$ cm^{-1} Å^8	[30]	2002	$C_8^{\Sigma}=3.45(37)\times10^6$
$C_8^{\Sigma}=2.805\times10^6$ a.u.	[32]	1995	$C_8^{\Sigma}=2.805\times10^6$

$$\frac{d\beta}{d\varepsilon}=-\frac{\sqrt{2\mu}}{h}\frac{c_n^{1/n}}{\epsilon^{(n+2)/2n}}\int_0^1\frac{x^{n/2}dx}{\sqrt{1-x^n}}$$
$$=-\frac{\sqrt{2\mu}}{h}\frac{c_n^{1/n}}{\epsilon^{(n+2)/2n}}\frac{\sqrt{\pi}}{n}\frac{\Gamma(1/2+1/n)}{\Gamma(1+1/n)}.$$

The integration of the level density gives (for $n\neq2$) the well-known LeRoy-Bernstein law

$$v_D-v=H_n^{-1}\epsilon^{(n-2)/2n},$$

$$H_n^{-1}=\frac{\sqrt{2\mu}}{\sqrt{\pi}}\frac{c_n^{1/n}}{\hbar(n-2)}\frac{\Gamma(1/2+1/n)}{\Gamma(1+1/n)},$$

where v_D is an integration constant whose integer part measures the level number of the molecular potential and H_n is a constant involving the molecular coefficient c_n. The noninteger part $\delta_D=v_D-E(v_D)$ gives (with a π factor) the phase difference between the last vibrational level defined with $v=E(v_D)$ and the dissociative state at $\epsilon=0$. The LeRoy-Bernstein formula is not valid for levels located very close to the dissociation limit. The criterion is usually defined relative to the v number, and the accuracy is given by $\sim1/\pi^2v^2$.

B. Asymptotic $(5s_{1/2}+5p_{1/2})0_g^-$ potential curve

In order to apply the LeRoy-Bernstein formula, the multipolar expansion of the $(5s_{1/2}+5p_{1/2})0_g^-$ molecular curve is analyzed. For the Hund case (c), the development of the potential, in the nonrelativistic case, is given by

$$V(R)=-A-\frac{4}{3}\frac{C_3^2}{AR^6}-\frac{2C_6^{\Pi}+C_6^{\Sigma}}{3R^6}-\frac{2C_8^{\Pi}+C_8^{\Sigma}}{3R^8},$$

where A is an energy constant connected to the $5p$ level fine structure by $\frac{3}{2}A=E(5p_{3/2})-E(5p_{1/2})$, and C_n coefficients are related to the atomic wave function. For instance, in the case of a rubidium atom, C_3 is given by $C_3=\langle5s|r|5p\rangle^2/3$.

For large values of R, the variation of the molecular potential is dominated by the term $-\frac{4}{3}(C_3^2/AR^6)$. In order to evaluate the terms in the development of the potential, we give in Tables II–IV the C_n values given in the literature or deduced from other coefficients. For the C_3 value, considering the first five values of Table II, we get the weighting mean value $C_3=8.949(10)$ a.u.

For all the next calculations, we take the following values: $A=158.398\,936\,62$ cm$^{-1}\equiv7.217\,186\,589\,2\times10^{-4}$ a.u. (deduced from Refs. [28,25]), $C_6^{\Pi}=8.05\times10^3$ a.u., $C_6^{\Sigma}=12.91\times10^3$ a.u., $C_8^{\Pi}=1.06\times10^6$ a.u., and $C_8^{\Sigma}=3.45\times10^6$ a.u. We

deduce $\frac{4}{3}C_3^2/A=1.4795\times10^5$ a.u.; $(2C_6^{\Pi}+C_6^{\Sigma})/3=0.0997\times10^5$ a.u., and $(2C_8^{\Pi}+C_8^{\Sigma})/3=1.86\times10^6$ a.u. With the notation defined in the previous section, $V(R)=D-c_6/R^6-c_8/R^8$, one gets $c_6=1.5792\times10^5$ a.u. and $c_8=+1.86\times10^6$ a.u. These values indicate than the $1/R^8$ term is 100 times smaller than the $1/R^6$ ones as soon as $R>34$ a.u. It corresponds to an energy ϵ ranging from 0 to $\sim10^{-4}$ a.u. (22 cm^{-1}). As a consequence, for the experimental range studied here, the LeRoy-Bernstein approach can be applied.

C. Lu-Fano graph

Let us now introduce the effective quantum number defined by $v^*=H_n^{-1}\epsilon^{(n-2)/2n}$, which naturally appears in the LeRoy-Bernstein formula. Its noninteger part, defined by $\delta=v^*-E(v^*)$, is therefore a constant value and is equal to δ_D.

This remark allows us to regard this quantity δ as the usual quantum defect that is currently used in any Rydberg state spectroscopy. In such studies, the quantum defect, deduced via a Rydberg law ($v^*=\sqrt{R/\epsilon}$, with R the Rydberg constant), is plotted versus the energy ϵ, in a so-called Lu-Fano graph [33]. Any deviation of δ to a constant value is the signature of a perturbation to the Rydberg law. The perturbations are generally due to core effects, or to some coupling with neighboring series.

For molecular physics, Lu-Fano graphs have recently been used to present and analyze calculations for Rb_2 and Cs_2 0_u^+ molecular states [34,35]. They illustrate coupling between two series, converging either to the $s+p_{1/2}$ limit or the $s+p_{3/2}$ limit with a coupling considered as a constant or dependent on the internuclear distance. For cesium, these models were then compared with experimental data [36]. In this paper, the Lu-Fano graph is applied to a 0_u^+ series, which is not coupled to another one. The approach in this case allows us to assess the relevance of the LeRoy-Bernstein formula.

Data recorded for the $(5s_{1/2}+5p_{1/2})0_g^-$ series, given in Table I, have been analyzed with this appraoch. The energy difference ϵ is deduced from the data by applying $\epsilon=D-E$. Due to the hyperfine coupling in the $5p_{1/2}$ atomic levels, the dissociation energy D could not be exactly defined. It has been chosen to be the atomic resonance $5s_{1/2}F=2\rightarrow5p_{1/2}F'=2$, whose energy is 12578.876 cm^{-1}. This arbitrary choice introduces a systematic error, $\Delta\epsilon_s$, on the ϵ value. $\Delta\epsilon_s$ is less than the hyperfine structure of the $5p_{1/2}$ level: $\Delta\epsilon_s<0.028$ cm^{-1}. Then, the effective quantum number is deduced by applying $v^*=(\epsilon/H_6^3)^{1/3}$ with $H_6^3=1.00410^{-3*}$ cm^{-1}. The error on v^* includes the experimental energy error, $\Delta E=0.01$ cm^{-1}, and the H_6^3 error, ΔH_6^3. Taking into account the data on C_3, C_6^{Π}, C_6^{Σ} given in Tables II–IV, one estimates $\Delta H_6^3/H_6^3=0.2\%$, and $\Delta v^*/v^*$ is evaluated by

$$\frac{\Delta v^*}{v^*}=\frac{1}{3}\left(\frac{\Delta E}{\epsilon}+\frac{\Delta H_6^3}{H_6^3}\right).$$

The numerical value is therefore $\Delta v^*/v^*=(0.01/\epsilon+0.002)/3$ for ϵ given in wave-number units. Adding the systematic error, the maximum error is therefore $(\Delta v^*/v^*)_M=(0.038/\epsilon+0.002)/3$. At last, the quantum defect δ is extracted and plotted versus the energy. The plot is shown in Fig. 3. Because the quantum defect is defined modulus 1, it might be convenient to add or substract one unit from the value to clearly show a variation law. The plot in Fig. 3 clearly exhibits a linear dependance of δ versus ϵ, which does not agree with the $\delta=\delta_D$ previously expected value.

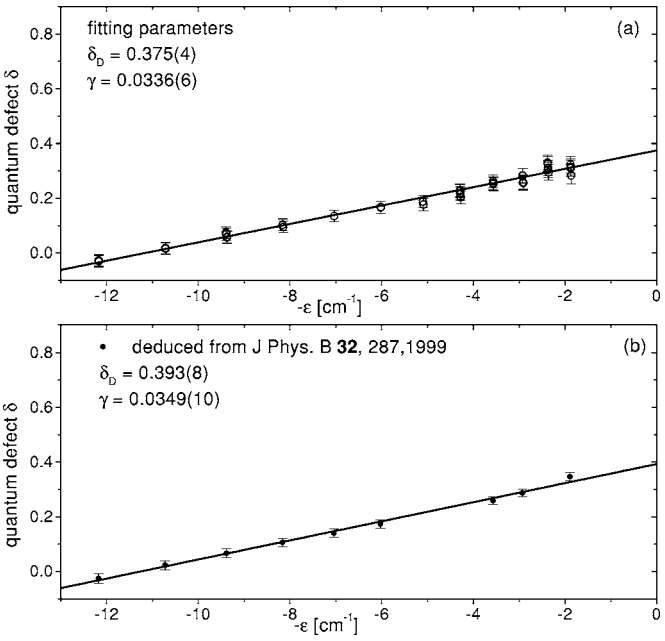

FIG. 3. Quantum defect versus the energy and the linear fit: (a) for data of Table I, (b) for data given in [13].

D. Improved LeRoy-Bernstein formula

It is fruitful to analyze the importance of the two main approximations in the LeRoy-Bernstein theory: (i) the use of the asymptotic potential $V(R)=D-c_n/R^n$, (ii) the extension of the integral for short values of R, allowing $R_-=0$. This analysis is done in Comparat's paper [23], including details of the calculation and orders of magnitude for the cesium case. Here, we point out the result established in [23] in Sec. II D, formula (13), by using a Taylor expansion. Within this approach, the improved LeRoy-Bernstein formula is shown to be

$$v_D-v=H_n^{-1}\epsilon^{(n-2)/2n}+\gamma\epsilon$$

with γ a parameter that globally includes core effects and correction due to the difference between the real potential and the considered asymptotic form.

This improved LeRoy-Bernstein formula is easily connected to the data analysis via $v^*=v_D-v-\gamma\epsilon$. Considering the order of magnitude of γ, the term $\gamma\epsilon$ is a small deviation to the LeRoy-Bernstein formula. Therefore, the quantum defect will vary as $\delta=\delta_D-\gamma\epsilon$, i.e., linearly versus the energy. A linear fit of the plot in Fig. 3(a) gives $\gamma=0.0336(6)$ $(cm^{-1})^{-1}$ and $\delta_D=0.375(4)$.

These values can be compared to those we deduced from already published data [13]. Taking into account the energy positions of $(5s_{1/2}+5p_{1/2})0_g^-J=2$ levels, we plot the quantum

defects [Fig. 3(b)] and deduce the fitting parameters $\gamma=0.0349(10)(\mathrm{cm}^{-1})^{-1}$ and $\delta_D=0.393(8)$, which are compatible with the previous ones.

In order to make a connection between the two parameters (γ,δ_D) and the characteristics of the molecular potential, i.e., the short-range description including the core effects and the location of the minimum, we propose to analyze the problem with two models: (i) a crude model including an infinite barrier at $R=R_c'$, a constant potential in the region $[R_c',R_c]$, and a variation as $-c_6/R^6$ for $R>R_c$; (ii) a harmonic potential for $R<R_c$ with a minimum localized at $R=R_e$ and a variation as $-c_6/R^6$ for $R>R_c$. For both models we apply the Bohr-Sommerfeld quantization to deduce the analytical expression of both parameters (γ,v_D). Then, a comparison with the (γ,v_D) experimental parameters allows us to deduce values for R_c', R_c, and R_e.

1. Model (i)

The molecular potential is assumed to be a constant potential $V(R)=V_e$ in the region $[R_c',R_c]$ with an infinite barrier at $R=R_c'$, and $V=D-c_n/R^n$ for $R>R_c$. The integral β is then expressed by

$$\beta=\frac{\sqrt{2\mu}}{\pi\hbar}\left[\int_{Rc'}^{R_c}\sqrt{E-V_e}dR+\int_{R_c}^{R_+}\sqrt{E-D+c_n/R^n}dR\right].$$

With the energy difference $\epsilon=D-E$, assumed to be small compared to $U=D-V_e$, and for $R_c(\epsilon/c_n)^{1/n}\ll 1$, the integral β can be expressed as

$$\beta=\frac{\sqrt{2\mu}}{\pi\hbar}\sqrt{U}(R_c-R_c')\left[1-\frac{\epsilon}{2U}\right]-H_n^{-1}\epsilon^{(n-2)/2n}+\frac{\sqrt{2\mu}}{\pi\hbar}\left[\frac{\sqrt{c_n}}{R_c^{(n-2)/2}}\frac{2}{(n-2)}+\frac{R_c^{(n+2)/2}}{\sqrt{c_n}}\frac{\epsilon}{(n+2)}\right].$$

As $\beta=v+\frac{3}{4}$, and the improved LeRoy-Bernstein formula being $v_D-v=H_n^{-1}\epsilon^{(n-2)/2n}+\gamma\epsilon$, one gets $\beta=\frac{3}{4}+v_D-H_n^{-1}\varepsilon^{(n-2)/2n}-\gamma\epsilon$, and therefore

$$v_D=-\frac{3}{4}+\frac{\sqrt{2\mu}}{\pi\hbar}\left[\frac{2\sqrt{c_n}}{(n-2)R_c^{(n-2)/2}}+\sqrt{U}(R_c-R_c')\right],$$

$$\gamma=\frac{\sqrt{2\mu}}{\pi\hbar}\left[-\frac{R_c^{(n+2)/2}}{(n+2)\sqrt{c_n}}+\frac{1}{2\sqrt{U}}(R_c-R_c')\right].$$

Assuming a continuity of the potential at $R=R_c$, i.e., $U=c_n/R_c^n$, the expressions of v_D and γ are the following:

$$v_D=-\frac{3}{4}+\frac{\sqrt{2\mu}}{\pi\hbar}\frac{\sqrt{c_n}}{R_c^{(n-2)/2}}\left[\frac{2}{(n-2)}+1-R_c'/R_c\right],$$

$$\gamma=\frac{\sqrt{2\mu}}{\pi\hbar}\frac{R_c^{(n+2)/2}}{\sqrt{c_n}}\left[-\frac{1}{(n+2)}+\frac{1}{2}(1-R_c'/R_c)\right].$$

In the case of the 0_g^- molecular curve, with a total number of levels evaluated [26] to 212, one deduces $v_D=212.375$. Considering $\gamma=0.0336(\mathrm{cm}^{-1})^{-1}$, and $n=6$, the solution of

$$v_D=-\frac{3}{4}+\frac{\sqrt{2\mu}}{\pi\hbar}\frac{\sqrt{c_6}}{R_c^2}\left[\frac{3}{2}-R_c'/R_c\right]=212.375,$$

$$\gamma=\frac{\sqrt{2\mu}}{\pi\hbar}\frac{R_c^4}{2\sqrt{c_6}}\left[\frac{3}{4}-R_c'/R_c\right]=0.0336\ (\mathrm{cm}^{-1})^{-1}$$

gives $R_c=17.91$ a.u. and $R_c'=0.9$ a.u.

2. Model (ii)

The molecular potential is assumed to be a harmonic potential $V(R)=V_e+B(R-R_e)^2$ in the region $R<R_c$ and $V=D-c_n/R^n$ for $R>R_c$. The integral β is then expressed by

$$\beta=\frac{\sqrt{2\mu}}{\pi\hbar}\left[\int_{Rc'}^{R_c}\sqrt{E-V_e-B(R-R_e)^2}dR+\int_{R_c}^{R_+}\sqrt{E-D+c_n/R^n}dR\right].$$

With the quantities defined by $\epsilon=D-E$, $U=D-V_e$, and $L=\sqrt{(U-\varepsilon)/B}$, and for $R_c(\epsilon/c_n)^{1/n}\ll 1$, the integral β can be expressed as

$$\beta=\frac{\sqrt{2\mu}}{\pi\hbar}\frac{U-\varepsilon}{2\sqrt{B}}\left\{\frac{\pi}{2}+\frac{(R_c-R_e)}{L}\sqrt{1-\frac{(R_c-R_e)^2}{L^2}}+\arcsin\left(\frac{(R_c-R_e)}{L}\right)\right\}-H_n^{-1}\epsilon^{(n-2)/2n}+\frac{\sqrt{2\mu}}{\pi\hbar}\left[\frac{\sqrt{c_n}}{R_c^{(n-2)/2}}\frac{2}{(n-2)}+\frac{R_c^{(n+2)/2}}{\sqrt{c_n}}\frac{\epsilon}{(n+2)}\right].$$

In the case of $\epsilon=D-E$, assumed to be small compared to U, a Taylor expansion leads to

$$v_D=-\frac{1}{2}+\frac{\sqrt{2\mu}}{\pi\hbar}\frac{\sqrt{c_n}}{R_c^{(n-2)/2}}\frac{2}{(n-2)}+\frac{\sqrt{2\mu}}{2\pi\hbar}\frac{U}{\sqrt{B}}\left\{\frac{\pi}{2}+\sqrt{\frac{B}{U}}(R_c-R_e)\sqrt{1-\frac{B(R_c-R_e)^2}{U}}+\arcsin\left(\sqrt{\frac{B}{U}}(R_c-R_e)\right)\right\}$$

$$\gamma=-\frac{\sqrt{2\mu}}{\pi\hbar}\frac{R_c^{(n+2)/2}}{\sqrt{c_n}}\frac{1}{(n+2)}+\frac{\sqrt{2\mu}}{2\pi\hbar}\frac{1}{\sqrt{B}}\left\{\frac{\pi}{2}+\arcsin\left(\sqrt{\frac{B}{U}}(R_c-R_e)\right)\right\}.$$

A continuity of the potential and its derivative at $R=R_c$ allow us to express v_D and γ as functions of R_c and R_e. In the case of $n=6$, with $R_e/R_c=\eta$ one gets

$$v_D=-\frac{1}{2}+\frac{\sqrt{2\mu}}{2\pi\hbar}\frac{\sqrt{c_6}}{R_c^2}\left\{1+(4-3\eta)\sqrt{\frac{1-\eta}{3}}\left\{\frac{\pi}{2}+\frac{\sqrt{3(1-\eta)}}{4-3\eta}+\arcsin\sqrt{\frac{3(1-\eta)}{4-3\eta}}\right\}\right\}$$

$$\gamma=\frac{\sqrt{2\mu}}{2\pi\hbar}\frac{R_c^4}{\sqrt{c_6}}\left\{-\frac{1}{4}+\sqrt{\frac{1-\eta}{3}}\left\{\frac{\pi}{2}+\arcsin\sqrt{\frac{3(1-\eta)}{4-3\eta}}\right\}\right\}$$

Solving $v_D=212.375$ and $\gamma=0.0336(\mathrm{cm}^{-1})^{-1}$ gives $R_c=17.7$a.u. and $R_e=12.5$a.u. These values, although deduced with simple models, are quite in agreement with the numerical potential curves. This method allows us to characterize the potential in the inner zone with only a few spectroscopic data in the long-range region.

IV. CONCLUSION

The experimental spectroscopy of 0_g^- molecular states converging to the $(5s_{1/2}+5p_{1/2})$ limit has been experienced and analyzed in an asymptotic region, where the molecular potential has a very simple form. Therefore, the LeRoy-Bernstein formula is applicable. We show that the Lu-Fano method can be coupled to the LeRoy-Bernstein formula, to extract the energy variation of the quantum defect. For the 0_g^- molecular states, we observe a linear variation of the quantum defect versus the energy, which is in agreement with an improved LeRoy-Bernstein formula. Using this approach (Lu-Fano graph and improved LeRoy-Bernstein formula), with a fitting procedure, we deduce the limit of the quantum defect at the zero-energy limit and the slope of the energy variation. The quantum defect at the zero-energy limit (multiplied by π) is the phase shift of the wave function at the dissociation limit. Furthermore, we show that both parameters—the quantum defect at the zero-energy limit and the slope of the energy variation—are connected to the molecular potential characteristics for short-range distances. With two simple models, we extract from the fitting parameters the localization of the barrier, the potential minimum, and the limit of validity of the asymptotic form.

The proposed method, applied here in a quite simple case, because the molecular curve is not coupled to other curves, can be generalized. In the case of the analysis of Rydberg atom spectroscopy, this method has been fruitful and should be taken up for the molecular domain. For example, it should be very effective in estimating the coupling between molecular potentials.

ACKNOWLEDGMENTS

We thank D. Comparat for discussions about the improved LeRoy-Bernstein theory and O. Dulieu for level energy calculations. We also thank A. Crubellier, C. Drag, E. Luc-Koenig, F. Masnou-Seeuws, and P. Pillet for helpful discussions. Laboratoire Aimé Cotton is associated with Université Paris–Sud.

[1] H. R. Thorsheim, J. Weiner, and P. S. Julienne, Phys. Rev. Lett. **58**, 2420 (1987).
[2] P. D. Lett, K. Helmerson, W. D. Phillips, L. P. Ratliff, S. L. Rolston, and W. E. Wagshul, Phys. Rev. Lett. **71**, 2200 (1993).
[3] W. C. Stwalley and H. Wang, J. Mol. Spectrosc. **195**, 194 (1999).
[4] R. J. LeRoy and R. B. Bernstein, J. Chem. Phys. **52**, 3869 (1970).
[5] R. A. Cline, J. D. Miller, and D. J. Heinzen, Phys. Rev. Lett. **73**, 632 (1994).
[6] H. M. J. M. Boesten, C. C. Tsai, B. J. Verhaar, and D. J. Heinzen, Phys. Rev. Lett. **77**, 5194 (1996).
[7] C. Gabbanini, A. Fioretti, A. Lucchesni, S. Gozzini, and M. Mazzoni, Phys. Rev. Lett. **84**, 2814 (2000).
[8] A. Fioretti, C. Amiot, C. M. Dion, O. Dulieu, M. Mazzoni, G. Smirme, and C. Gabbanini, Eur. Phys. J. D **15**, 189 (2001).
[9] M. Kemmann, I. Mistrik, S. Nussmann, H. Helm, C. J. Williams, and P. S. Julienne, Phys. Rev. A **69**, 022715 (2004).
[10] J. D. Miller, R. A. Cline, and D. J. Heinzen, Phys. Rev. Lett. **71**, 2204 (1993).
[11] J. R. Gardner, R. A. Cline, J. D. Miller, D. J. Heinzen, H. M. J. M. Boesten, and B. J. Verhaar, Phys. Rev. Lett. **74**, 3764 (1995).
[12] C. C. Tsai, R. S. Freeland, J. M. Vogels, H. M. J. M. Boesten, B. J. Verhaar, and D. J. Heinzen, Phys. Rev. Lett. **79**, 1245 (1997).
[13] H. M. J. M. Boesten, C. C. Tsai, D. J. Heinzen, A. J. Moonen, and B. J. Verhaar, J. Phys. B **32**, 287 (1999).
[14] H. M. J. M. Boesten, C. C. Tsai, J. R. Gardner, D. J. Heinzen, and B. J. Verhaar, Phys. Rev. A **55**, 636 (1997).
[15] A. P. Mosk, M. X. W. Reynolds, T. W. Hijmans, and J. T. M. Walraven, Phys. Rev. Lett. **82**, 307 (1999).
[16] W. I. McAlexander, E. R. I. Abraham, N. W. M. Ritchie, and R. G. Hulet, Phys. Rev. A **51**, R871 (1995).
[17] E. R. I. Abraham, N. W. M. Ritchie, W. I. McAlexander, C. J. Williams, H. T. C. Stoof, and R. G. Hulet, J. Chem. Phys. **103**, 7773 (1995).
[18] L. P. Ratliff, M. E. Wagshul, P. D. Lett, S. L. Rolston, and W. D. Phillips, J. Chem. Phys. **101**, 2638 (1994).
[19] H. Wang, P. L. Gould, and W. C. Stwalley, J. Chem. Phys. **106**, 7899 (1997).
[20] C. Drag, B. Laburthe Tolra, O. Dulieu, D. Comparat, M. Vatasescu, S. Boussen, S. Guibal, A. Crubellier, and P. Pillet, IEEE J. Quantum Electron. **36**, 1378 (2000).
[21] C. M. Dion, C. Drag, O. Dulieu, B. Laburthe Tolra, F. Masnou-Seeuws, and P. Pillet, Phys. Rev. Lett. **86**, 2253 (2001).
[22] M. Pichler, H. Chen, and W. C. Stwalley, J. Chem. Phys. **121**, 1796 (2004).
[23] D. Comparat, J. Chem. Phys. **120**, 1318 (2004).
[24] H. Wang, P. L. Gould, and W. C. Stwalley, Phys. Rev. A **53**, R1216 (1996).
[25] G. P. Barwood, P. Gill, and W. R. A. A. Rowley, Appl. Phys. B **53**, 142 (1991).
[26] O. Dulieu (private communication).
[27] U. Volz and H. Schmoranzer, Phys. Scr., T **T65**, 48 (1996).
[28] J. Ye, S. Swartz, P. Jungner, and J. Hall, Opt. Lett. **21**, 1280 (1996).
[29] J. E. Simsarian, L. A. Orozco, G. D. Sprouse, and W. Z. Zhao, Phys. Rev. A **57**, 2448 (1998).
[30] R. F. Gutteres, C. Amiot, A. Fioretti, C. Gabbanini, M. Mazzono, and O. Dulieu, Phys. Rev. A **66**, 024502 (2002).
[31] M. S. Safronova, W. R. Johnson, and A. Derevianko, Phys.

Rev. A **60**, 4476 (1999).
[32] M. Marinescu and A. Dalgarno, Phys. Rev. A **52**, 311 (1995).
[33] K. T. Lu and U. Fano, Phys. Rev. A **2**, 81 (1970).
[34] V. Kokoouline, O. Dulieu, and F. Masnou-Seeuws, Phys. Rev. A **62**, 022504 (2000).
[35] V. N. Ostrovsky, V. Kokoouline, E. Luc-Koenig, and F. Masnou, J. Phys. B **34**, L27 (2001).
[36] V. Kokoouline, C. Drag, P. Pillet, and F. Masnou-Seeuws, Phys. Rev. A **65**, 062710 (2002).